Manuscript no. WES-2025-185

February 19, 2026

We thank the reviewers for their time and thoughtful feedback on our manuscript. Their comments have been instrumental in improving the quality of the paper. Our detailed responses to reviewers' questions are provided below. The reviewer's comments are in *italic*, our response is in regular font, and changes to the manuscript are highlighted in blue.

Reviewer #1

The authors present an experimental wind-tunnel study on the wake behaviour of a statically yawed porous disc subjected to veered inflow. Stereoscopic particle image velocimetry is used to investigate the spatial evolution of the wake across different planes and streamwise distances, including the available power, momentum budgets, and vorticity fields.
I find the manuscript very well written, with a sound analysis of wind-energy flows based on a state-of-the-art facility and experimental technique. I therefore consider the manuscript suitable for publication, provided that the authors address the following minor remarks.

Reply: We thank the reviewer for finding our manuscript well-written and acknowledging our work. Please find below the point-by-point responses to your questions.

Minor comments

1. *I did not find the distance between the porous disc and the grids, although it is mentioned that the disc is placed quite close to them. As the flow near the grid is not fully developed, what may generate spurious anisotropy and turbulence production effects, could the authors comment further on the flow properties at the disc position? This is partially discussed in Section 2.6, but such near-field effects may affect the reproducibility and applicability of the results.*

Reply: We thank the reviewer for this comment. We clarify that the porous disc is positioned approximately 20 cm ($\approx 2D$) downstream from the exit of the wind veering vanes (where $D = 10\ cm$). We positioned the disc relatively close to the tunnel exit because the tunnel has an open jet, which limits the maximum downstream distance at which stable wake measurements can be obtained before flow quality deteriorates. Regarding flow quality: the reviewer is correct in pointing out that the flow around the grid has not completely developed, and the "spurious anisotropy" is indeed observed (see Fig. 1). Our analysis (Fig. 1) indicates that the reference uniform inflow (without veering vanes) exhibits inherent anisotropy, with the average lateral (σ_v/σ_u) and vertical (σ_w/σ_u) ratios of 0.63 and 0.69, respectively, at the disc location. On the other hand, the introduction of the veering vanes increases lateral anisotropy locally within the shear layers of the vane wakes, reaching values up to 1.5. This is an unintended consequence and a limitation of this experimental setup. However, it is important to note that this effect is spatially localized. A threshold-based analysis indicates that these regions of elevated lateral anisotropy ($\sigma_v/\sigma_u > 1.1$) occupy only 9 % and 12 % of the disc swept area for the 10° and 20 ° wind veer cases, respectively. It is noted here that the lateral anisotropy does not completely disappear and some localized patches are still observed, even at $x/D = 7$. Furthermore, the vertical anisotropy remains largely unaffected, which is consistent with the primary role of the veering vanes in inducing directional (lateral) shear rather than the vertical shear. Overall, while the vane-based approach successfully

generates the desired wind veer, it introduces localized excess lateral turbulence. Additionally, even with the anisotropy, the values of the standard deviation of streamwise fluctuations remains low; the turbulence intensity ($TI = \sigma_u/U_{ref}$) at the disc position is approximately 2.6 % for the uniform inflow and remains bounded below 3 % for the veered inflow of 10°.

We have mentioned the position of the porous disc in Section 2.2 (Line 179–182) of the revised manuscript and added the following lines:

The porous disc is positioned ≈ 20 cm downstream of the exit of the wind veering vanes. The disc was placed relatively close to the tunnel exit because the facility operates in an open-jet configuration, which limits the maximum downstream distance at which stable wake measurements can be obtained before flow quality deteriorates.

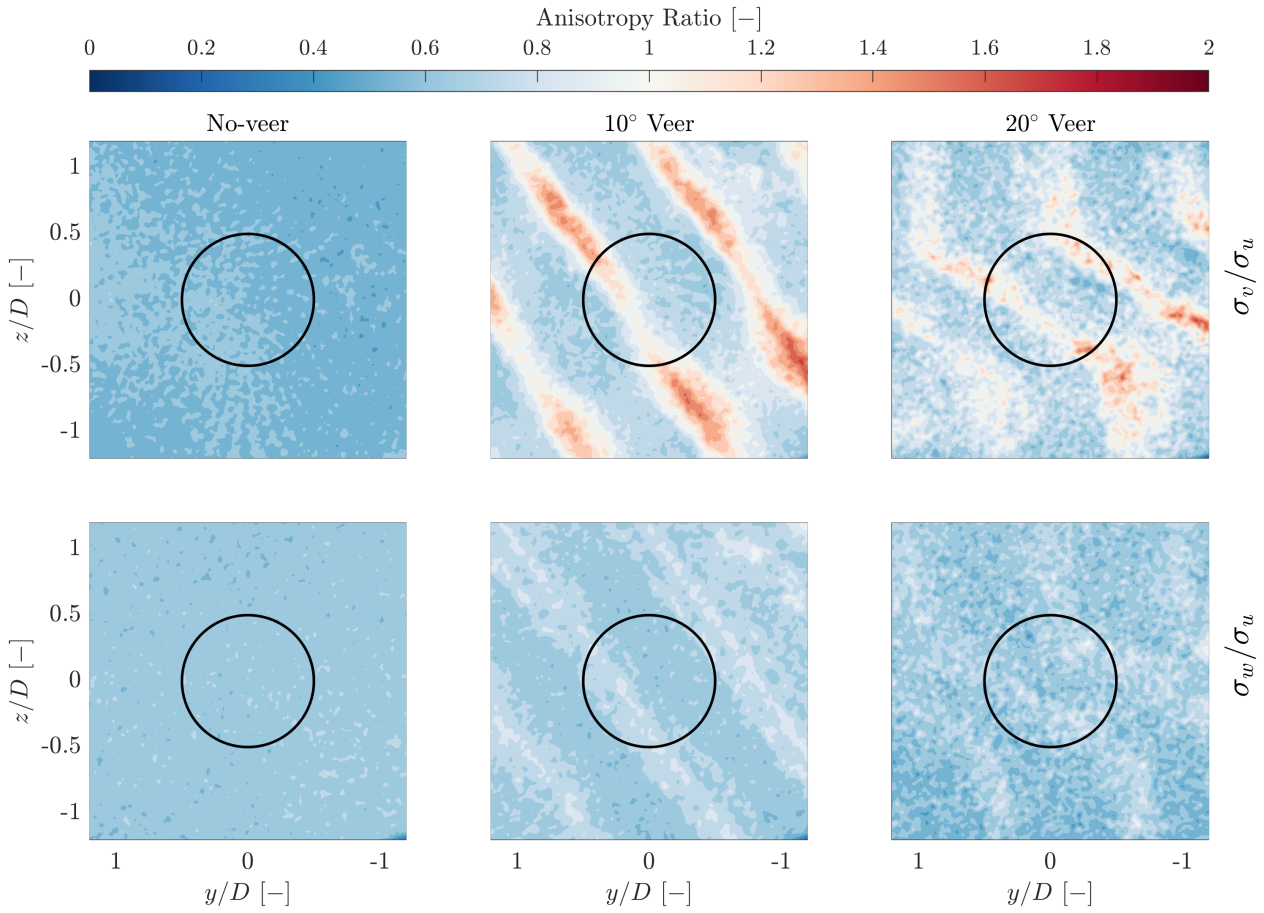

Figure 1: Lateral (top panel) and vertical (bottom panel) anisotropy ratio for the three cases (in the absence of porous disc). The black circle represents the projection of the non-yawed disc.

2. *The authors discuss the PIV spatial resolution (line 190), but it is not clear to me what the final resolution of the fields is, including the overlap for the smallest interrogation windows. In addition, did the authors verify that 100 vector fields are sufficient for convergence? Some terms in the budgets from equations 6 and 7 may require larger datasets to converge properly.*

Reply: Thanks to the reviewer for this comment. For the first part of the question, the final interrogation window size was 64 × 64 px^2 (9×9 mm^2). We employed a 50 % overlap during

processing, resulting in a final vector grid resolution of 32 pixels (4.5 mm). Secondly, to check whether 100 images are sufficient for the convergence of second-order statistics, we performed a cumulative convergence analysis of the TKE at one point of high turbulence intensity within the wake shear layer at $x = 3D$ for the case of no veer and no yaw. The evolution of TKE with the number of images is presented in Fig. 2a, and the relative convergence error is shown in Fig. 2b. The data indicates that the TKE estimates stabilize satisfactorily with residual fluctuations dropping below 5 % after approximately 80 images. As an additional verification, we also estimated the standard uncertainty associated with the turbulent kinetic energy U_k described in Sciacchitano and Wieneke (2016):

$$U_k = \sqrt{\overline{u'u'}^2 + \overline{v'v'}^2 + \overline{w'w'}^2} \cdot \sqrt{\frac{1}{2N}} \tag{1}$$

Therefore, the error in TKE computation is of the order of $\sqrt{\frac{1}{2N}}$. For $N = 100$, the error in TKE is around 7 %. Fig. 3 shows the spatial distribution of standard uncertainty in TKE for the three inflow cases for the non-yawed condition of the disc at $x/D = 3$. Consistent with the discussion on TKE in Section 3.4, the TKE is concentrated more in the bottom half of the disc, presumably due to a greater influence of the tower wake.

In the revised manuscript, we have mentioned the final resolution of the PIV fields in Section 2.4 (Line 227–228). We have also added the above discussion on standard uncertainty associated with the TKE in Section 2.5 (Line 258–262).

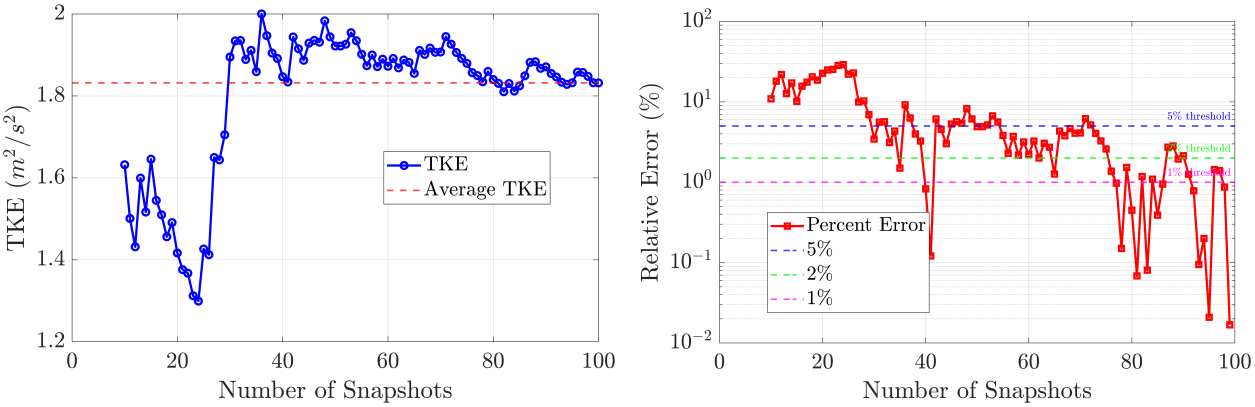

(a) Variation of TKE with number of images

(b) TKE convergence error plot

Figure 2: Convergence error plot of the PIV data

3. *In Figure 5a and others, local velocities appear to exceed the inflow velocity. Is this correct, or an artefact of the colormap? If such higher velocities are indeed observed, this may imply blockage effects caused by the proximity of the plates to the tunnel exit.*

Reply: We believe it is just an artefact of the visualization in regions that locally have a velocity slightly higher than U_{ref}. We have investigated this and can confirm that these values (approximately 2 % higher than the freestream wind speed) are primarily a result of the normalization procedure rather than significant blockage effects. To clarify, U_{ref} is defined as the area-averaged velocity magnitude ($\overline{U} = \sqrt{u^2 + v^2 + w^2}$) over the disc projection area in the absence of the porous

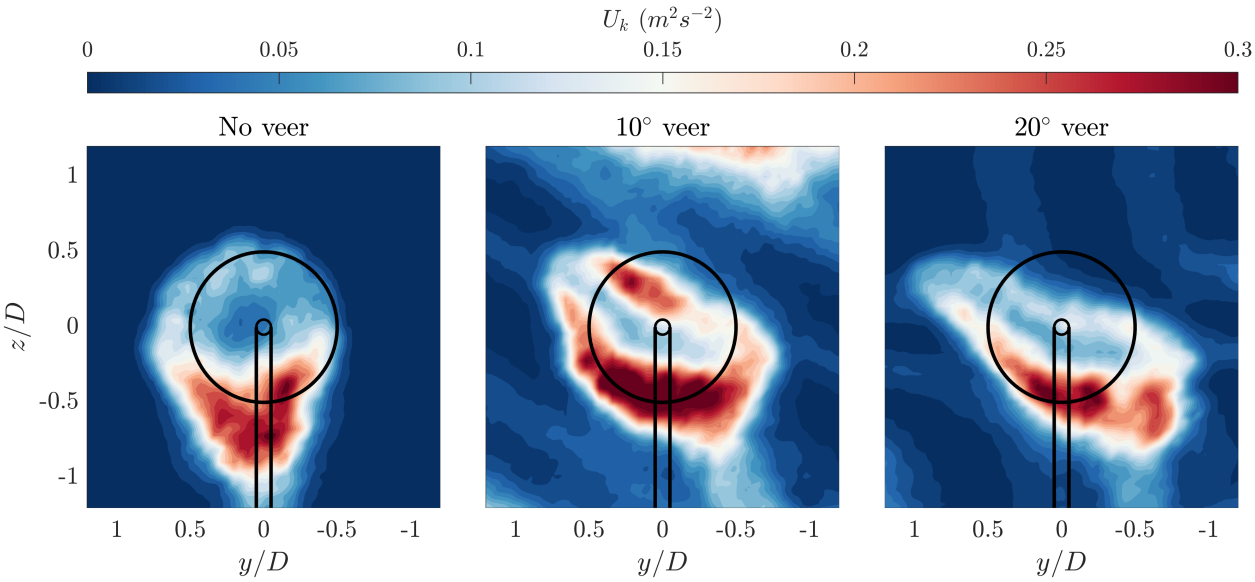

Figure 3: Spatial distribution of the TKE uncertainty at $x/D = 3$ for the three inflow cases for the non-yawed condition.

disc. Because the inflow is not perfectly uniform—particularly in the wind veer cases—the local velocity at some points naturally fluctuates above and below this mean value. It is perhaps because of this reason that the local velocity seems to be higher than the freestream velocity. We have added the following sentence at Line 271 in the revised manuscript.

U_{ref} is defined as the area-averaged velocity magnitude ($\overline{U} = \sqrt{u^2 + v^2 + w^2}$) over the disc projection area in the absence of the porous disc.

4. *In Bastankhah et al., JFM 2020 (already discussed by the authors), a model is presented to describe the displacement of the centroid of a wake behind a yawed wind turbine. Even though only three streamwise distances are available for the yaw-only case, did the authors consider verifying whether their results are consistent with this model?*

Reply: Thanks to the reviewer for this suggestion. If we are not mistaken, the reviewer is probably referring to Bastankhah et al. (2022). In that case, we have not compared our experimental results with the vortex sheet-based curled wake model yet. This is because the primary goal of this work is to experimentally study the effects of wind veer on wind turbine in a laboratory setting, as stated in the introduction. Certainly, the data will be useful and available for validation of these types of reduced-order models, which is also an ongoing work in our research group.

5. *While the introduction is clear and well written, there appear to be issues with the use of textual and parenthetical citations. Moreover, the literature review is extensive and precise. Still—this is only a suggestion—the authors may wish to mention that another avenue currently under development concerns the use of active grids to generate veered inflows.*

Reply: In the revised manuscript, we have fixed the improper citations issue. Regarding the use of active grids for generating veered inflow, we have added the following text in the revised manuscript in Section 2.2 (Lines 189–195):

Another promising avenue for generating veered inflow is the use of active grids (Neuhaus et al., 2021). While these grids are commonly used for generating shear flows, gusts, and homogeneous and isotropic turbulence, they theoretically possess the capability to generate wind veer. By switching from standard counter-rotating shaft protocols—which are designed to neutralize deflection—to co-rotating adjacent shafts, the system could effectively steer the flow. Alternatively, Multi-fan wind tunnels (MFWTs) offer a state-of-the-art solution that overcomes the mechanical constraints of physical grids. MFWTs can achieve directional flow by employing multi-directional driving models, which selectively activate fan pairs oriented toward the desired flow angle (Rajasekara Babu et al., 2025).

6. *Despite the authors' efforts, Figure 2 remains difficult to read. Is it possible to edit the background of the room to remove spurious objects?*

Reply: Thanks to the reviewer for the suggestion. In the revised manuscript, we have replaced the old figure with a new one after removing the background and spurious objects. We have also added the geometric details of the porous disc. Please see Fig. 2 of the revised manuscript on Page 7.

Reviewer #2

This work deals with an interesting topic: how the wake of a wind turbine is affected by veer and yaw. As yawing is a key issue in wind farm optimisation, this topic is highly relevant. The authors take an experimental approach to this topic, using a porous disc in a wind tunnel for which they have constructed a veering grid. This is an innovative experimental approach. Their main finding is that veering leads to faster wake recovery. The paper is well structured. Overall, this paper should definitely be published, but several points should first be clarified.

Reply: We thank the reviewer for acknowledging our work and finding the experimental approach innovative. Please find our responses to your questions below.

Specific comments

1. (a) *My main concern is the validity of their key conclusion that veering leads to faster wake recovery. The analysis of the wake data could be improved. I suggest they clearly demonstrate that veering causes more than advection of the wake in different directions. In other words, the recovery deviates from the simple additive effect of veer and yaw (as discussed in part in Mohammedi's citation).*

Reply: We thank the reviewer for this comment. Based on our understanding of your suggestion, we constructed a simple advection model to isolate the geometric effect of veer from any enhanced recovery mechanisms, and compared the model results against our measurement data (see Fig. 4). The procedure to make the middle contour in Fig. 4 is as follows: we took the entire velocity field from the WV0Y0 case at $x/D = 5$ and laterally displaced the velocity profile at each height by $\Delta y(z) = x \cdot tan(\alpha(z))$, where $\alpha(z)$ is the local veer inflow angle obtained from the inflow characterization measurements of the 10° veered case. This produces a predicted wake shape under the assumption that veer acts purely as passive advection. Then we compare this full shifted field against the actual wake measurement under veered inflow (rightmost contour in Fig. 4).

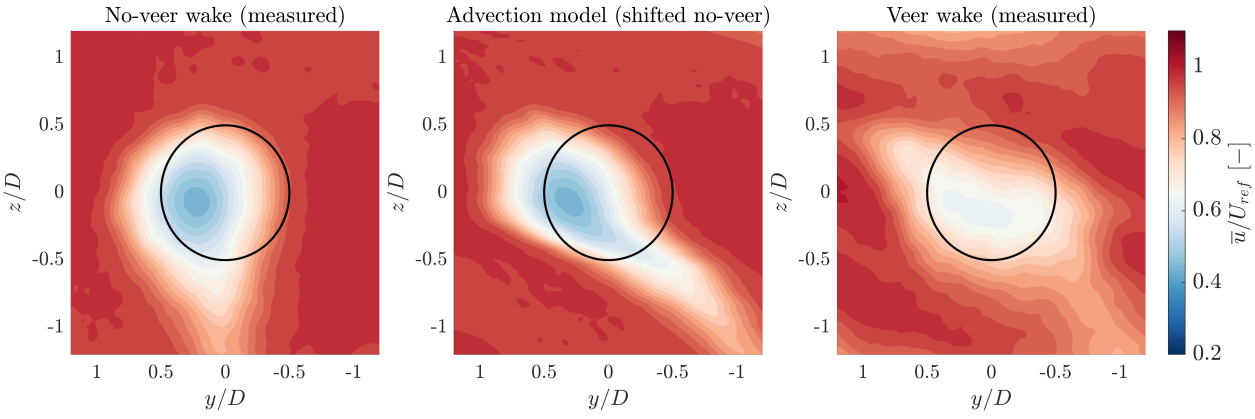

Figure 4: Comparison of a simple model advection with the experimental results of veer wake at $x/D = 5$. The leftmost plot corresponds to the case of WV0Y0, the middle plot is obtained from the simple advection model, and the rightmost plot is the measured case of WV10Y0.

As can be seen from the Fig. 4, wind veer is not just displacing the wake laterally, but also aiding in faster recovery of the wake. A similar approach was also adopted by Churchfield and Sirnivas (2018) (see discussion on pp. 5 and associated Fig. 7 of their paper), where the authors

advect a vertical line of points using the inflow profile and measure the angle of the resulting tilted line ("expected skew"). Then they find the lateral position of the wake deficit minimum at each height and measure that angle ("actual skew"), and compare the two angles.

We have added this simple advection model comparison with measurements in Appendix C in the revised manuscript.

1. (b) *Due to the uncertainties arising from imperfect wind tunnel flow (see below), the wake quantities (mean velocity, TKE, wind power, etc.) should be analysed using an integral over the entire wake area, including symmetric, skewed and curled cases. Variation in thresholds to define the wake can indicate experimental precision. Such an analysis is very important for their power considerations. As detailed below, the power of a turbine in a wake should also be averaged over different y positions. Even a simple linear translation in a different direction by veer would automatically lead to faster power recovery in a fixed rotor plane. It is important to quantify the difference between such a simple advection model and the experimental data, only than one can conclude that a faster recovery is observed.*

Reply: We thank the reviewer for this constructive comment and the suggestion to perform an integral analysis. We performed the suggested integral analysis of the momentum deficit. We define the integrated wake deficit as $M_x = \iint \Delta u \; dA/U_{ref}A_w$, where Δu is the streamwise wake deficit, U_{ref} is the reference velocity of the inflow case, and A_w is the wake area (identified using the wake threshold). Fig. 5 presents the integrated deficit for two different wake boundary thresholds ($\overline{u}/U_{ref} = 0.85$ and 0.9) to ensure robustness. For the non-yawed cases and different veer scenarios, it can be seen that the total momentum deficit decays faster in the veered case compared to the non-veered baseline, indicating active recovery beyond simple steering. The accelerated decay reinforces our primary conclusion that wind veer indeed helps in wake recovery, by bringing fresh momentum from the freestream into the wake. The trends remain consistent when choosing different wake thresholds. As expected, yaw accelerates the wake recovery even further, as evidenced by the dashed lines, which are consistently below the solid lines. This is also consistent with the findings of momentum budget analysis in Section 3.3 in the original manuscript (see bar plot in Fig. 14 in the revised manuscript, which shows term II ($\langle -\frac{\overline{w}}{\overline{u}}\frac{\partial \overline{u}}{\partial z}\rangle$) for veered cases being significantly higher than the no-veer case).

We have focused the integral analysis on mean velocity and available power because these quantities directly quantify the state of wake recovery. While TKE drives this process, the available power analysis provides the definitive proof that wake has re-energized. Regarding the available power, we must point out that we have already shown the integral analysis of the available power variation in Section 3.5 in the original manuscript. More details about this can be found in one of your later comments.

In the revised manuscript, we have added the integrated momentum deficit discussion in Section 3.1 (Lines 374–387). We have also added the plot corresponding to the wake threshold $\overline{u}/U_{ref} = 0.9$ (please see Fig. 9 of the revised manuscript).

1. (c) *I also miss a quantitative comparison of the experimental results with the models of Mohammadi et al. (2022) and Narasimhan et al. (2025).*

Reply: As also mentioned in Reviewer # 1 comment # 4, we would like to reiterate that model comparison of our experimental results is outside the scope of the current work.

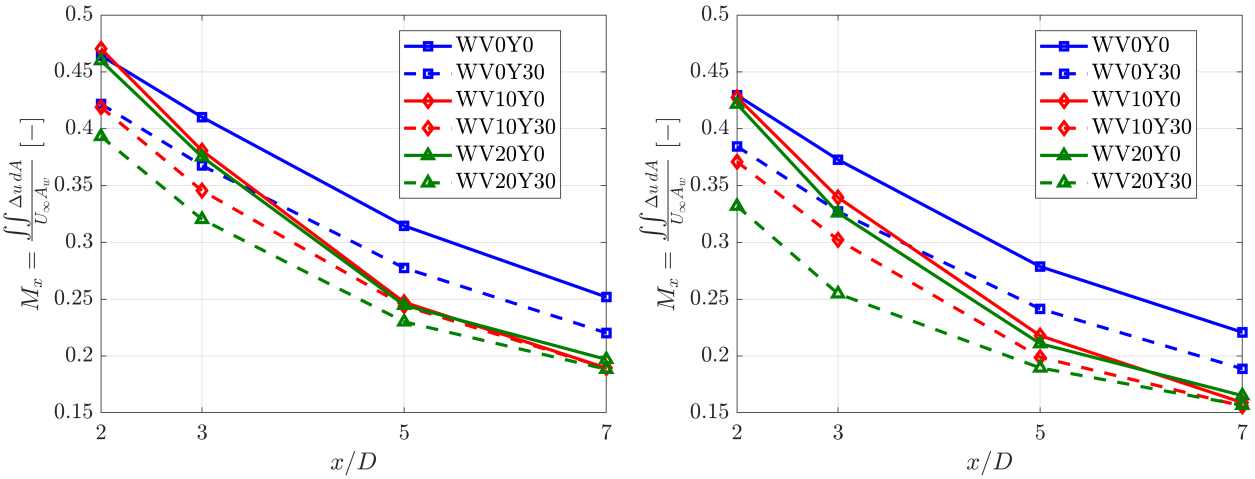

(a) $\overline{u}/U_{ref} = 0.85$ (b) $\overline{u}/U_{ref} = 0.90$

Figure 5: Integral analysis of the mean wake deficit computed in the wake area for different thresholds that define the wake area

2. (a) *Another serious issue is the inhomogeneity of the wind tunnel, which causes the V0Y0 case to drift to the left (see Fig. 5b).*

Reply: We thank the reviewer for this important observation. After talking to the lab technicians and upon further analysis of the flow characterization measurements, we have identified a systematic lateral deflection in the wind tunnel inflow, particularly in the central region. Characterization of the flow in the clean case reveals a mean crossflow velocity component of approximately 0.23 m/s in the disc region, along with a persistent mean vertical velocity of 0.20 m/s throughout the imaging plane. This can be observed in the flow characterization contours of spanwise and vertical velocity components in Fig. 6 for the reference uniform inflow case. Contrary to our earlier hypothesis about the laser misalignment, the "drift" in the wake of the WV0Y0 case occurs largely because of the non-uniform inflow in the wind tunnel. This lateral and vertical deflection was recently observed in some other experiments of our colleagues. Unfortunately, this problem was realized much later after the current experimental campaign. Nevertheless, the wind tunnel-induced deflection does not affect our primary conclusions regarding the impact of wind veer on wake structure, as the veer-induced effects are captured relative to this reference uniform inflow condition.

In the revised manuscript, we have added the following note about this in Section 3.1 (Lines 319–322), along with the Fig. 6 in Appendix A.

Notably, across all cross-stream planes in the non-yawed case under uniform inflow (see Fig. 5b), the wake consistently exhibits a lateral displacement toward the left. This is attributed to the inhomogeneity in wind tunnel inflow, which results in a systematic lateral deflection, particularly in the central region of the tunnel (see Appendix A for flow characterization contours).

2. (b) *The periodic structures caused by the veering grid seen in Figures 6a and 7a should also be discussed more critically. I am not convinced that the results are not heavily influenced by this imperfect experimental setup. This is a clear drawback of the experimental design of this work. I expect an own subchapter on this point.*

Reply: Regarding the periodic structures in the wake for veered inflow, we acknowledge that generating veer using the way we have done can result in the formation of the wake of the vane (leading to these periodic structures) and might have some effect on the results presented here, but the effect is localized and not large enough to alter the general findings of this work. For instance, the maximum velocity deficit due to the porous disc (Δu_{wake}) at $x/D = 3$ for the WV0Y0 case is $0.65 \cdot U_{ref}$, whereas deficit due to the vane (Δu_{vane}) at the same location in the absence of the porous disc is $0.05 \cdot U_{ref}$. This confirms that the periodic structures act as a passive background turbulence source rather than a driver of the mean wake shape. The reviewer is also requested to refer to the lateral and vertical anisotropy ratio we discussed in Reviewer #1 comment #1.

In the revised manuscript, we have added some parts of the above discussion in Section 3.1 (Lines 355–361))

Regarding experimental limitations: Nevertheless, as this is the first study in the literature to investigate wind veer effects in a laboratory setting, certain limitations of the experimental setup are unavoidable. We have addressed these transparently in the new Section 4 (Lines 589–613) "*Limitations of the experimental setup and future work*," as requested by the reviewer. We summarize some limitations here briefly and the ways to overcome it. One major drawback of using the veering vanes is the wake of the vanes, which creates a wake deficit region that has a slight influence on the wake shape in the presence of the porous disc. Another disadvantage is that the variation of wind veer is not completely linear with height, but rather is "wavy", as shown in the contours of Fig. 7. The variation with height becomes much more uniform and linear at farther downstream distances (not shown here). However, due to space restrictions, it could not be done in our experiments. Further research is needed to improve the veer-generating ability of these vanes. For instance, zigzag tapes could be employed so that the airflow remains attached to the steepest parts of the airfoil, which can prevent the formation of laminar separation bubbles. Optimization of vane spacing and solidity should be investigated as ways to homogenize the flow field. Gauze screens could also be used to break the asymmetry in lateral wind veer profile. Apart from the improvements in the wind veering vane geometry, future work should also use a miniature rotating wind turbine model, and the rotational direction of the turbine should also be investigated. Studies by Englberger et al. (2020a,b) have shown a crucial role played by turbines that rotate in CCW direction.

3. *I miss a discussion of the choice of yaw angles which go only in the direction of veer. I think it is discussed in the literature which consequence a yawing in the other direction will have. This should be included in the paper at least as a discussion.*

Reply: Thanks to the reviewer for this comment. Indeed, the choice of yaw angles can clearly have an impact on the wake properties. Previous studies, such as by Narasimhan et al. (2025), did show that the negative yaw can result in reduced wake deflection due to opposing effects of veer and yaw. As a result of this, the wake is still within the frontal projection of the rotor. In another LES study of a wind farm, Archer and Vasel-Be-Hagh (2019) found that negative yaw misalignment causes power losses in the northern hemisphere, primarily due to Coriolis force effects. Moreover, our decision to focus on positive yaw was also motivated by our own simulations of the NREL 5MW turbine operating in different stable boundary layers, where the negative yaw angle of $-30°$ provided negligible benefits in available power for the downstream turbines compared to the positive angles (under review in another journal). In the revised manuscript, we have added the following lines in Section 2.3 (Lines 201–206):

In this study, yaw misalignment is applied only in the direction of the inflow veer (positive yaw). This is motivated by the fact that spanwise velocity induced by negative yaw angles counteracts the

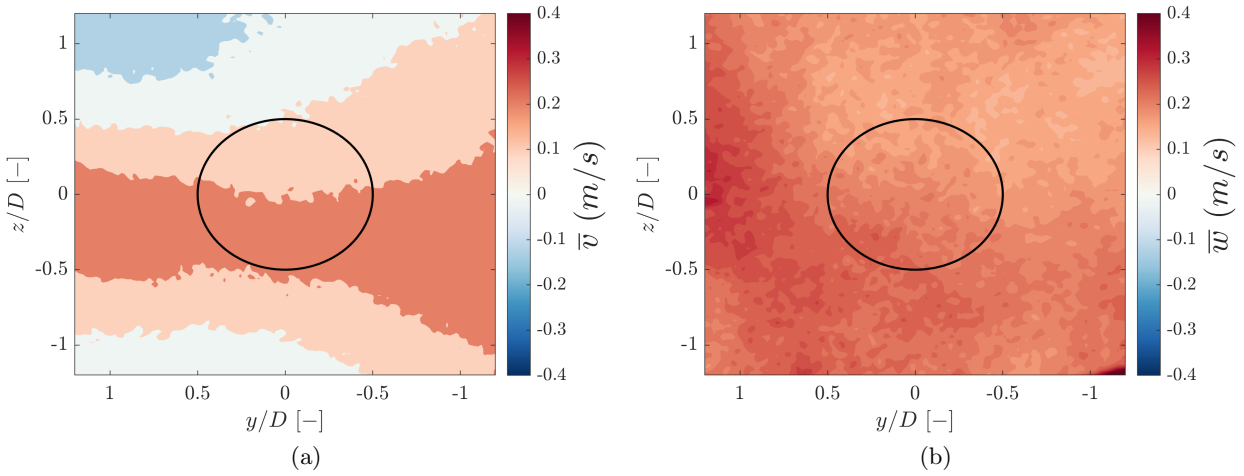

Figure 6: Flow characterization contours in the $yz-$plane for the clean case in the absence of porous disc: (a) Spanwise velocity; (b) Vertical velocity.

direction of veer that can restrict the wake to rotor frontal projection (Narasimhan et al., 2025), whereas positive yaw acts constructively with veer to enhance wake deflection (Vollmer et al., 2016). Other LES-based wind farm studies also show that negative yaw results in overall power losses in the northern hemisphere (Archer and Vasel-Be-Hagh, 2019).

4. *The paper is formally OK, but the presentation of results in figures should be revised. The same notation as that introduced for Fig. 16 should be used throughout the work. The presentation in the figures should also follow the same scheme wherever possible, e.g. yaw in the y-direction and veer in the x-direction, starting with yaw 0 veer 0 and the bar of colouring to the right.*

Reply: Thanks to the reviewer for this suggestion. Apart from Fig. 16, only Fig. 10 had line plots. We have modified that plot to match the color scheme used in Fig. 16. Moreover, we have now presented results in a consistent manner—yaw variation vertically and veer variation horizontally.

5. *The citation (Englberger, WES 5, 1359 (2020)) showing that the turbine's rotation plays a role should be mentioned, may be also as a further detail to be investigated in future. It could be added close to line 104, where the choice of a non-rotating porous disc is mentioned.*

Reply: Thanks to the reviewer for pointing out this study. We have included the citation (Englberger et al., 2020a,b) in the revised manuscript in the new Section 4 titled "*Limitations of the experimental setup and future work*" at Lines 610–613. We believe it is more appropriate here rather than in the introduction.

Minor comments and some more details:

1. *Fig 1(an and b): The sketches how the laser is positioned is in my opinion wrong. The laser beam is aligned with the plane of the light sheet. I see a discrepancy to Fig 2 - isn't here the laser below the flowing is directed in z direction. Your definition of x=0D is the location of the disc (line 167)- which does not fit to Fig 1 a.*

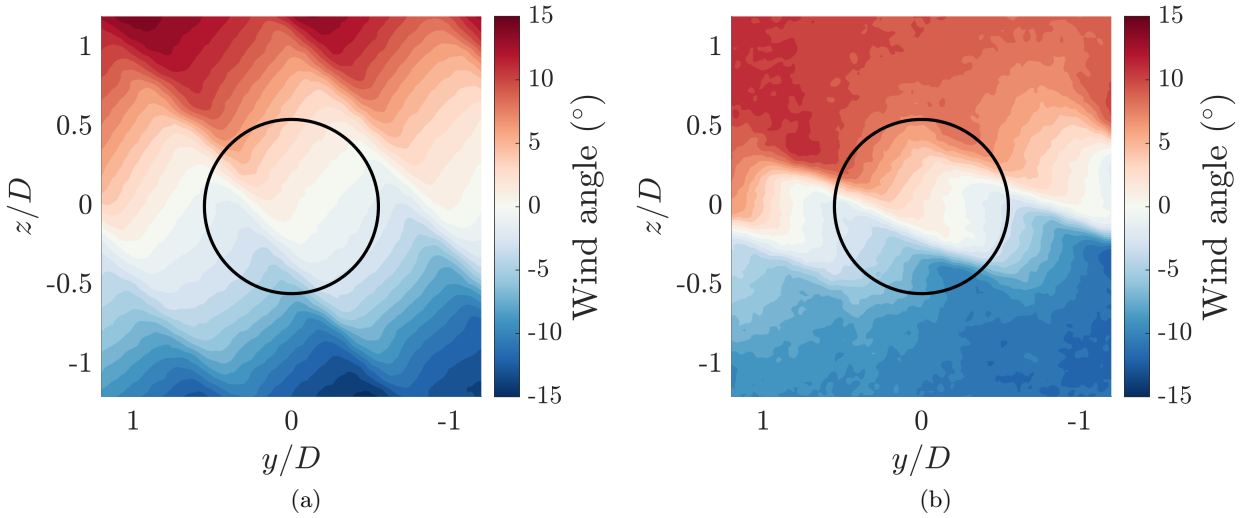

Figure 7: Flow characterization contours of variation of wind veer in the $yz-$plane at $x/D = 0$ (a) Veer 10°; (b) Veer 20°.

Reply: We thank the reviewer for pointing out this potential source of confusion. The discrepancy arises from the way the yaw motion is implemented in the physical experiment and how the coordinate system is subsequently treated in post-processing. In the laboratory setup, the disc is yawed with respect to the y-axis of the coordinate system shown in Fig. 2. The tower attached to the rotation stage is mounted on the side of the vertical beam (marked ② in Fig. 2). As a result, the wake is physically deflected upward, i.e. in the z-direction. With this in mind, Fig. 1(a) is consistent with the experimental setup: when viewed from the top, the laser sheet lies in the plane of the light sheet and therefore appears as a line. To measure the streamwise wake plane, we rotate the rotation stage by 90° and we acquire data in the xz-plane of the laboratory coordinate system (which is equivalent to the xy-plane after a coordinate transformation). For the data analysis and presentation of results, we follow the standard convention used in the literature, where the tower is aligned with the z-direction and yaw occurs about the z-axis, resulting in wake deflection in the y-direction. Accordingly, the coordinate system is rotated during post-processing to match this convention. We have added an explicit note clarifying this distinction between the laboratory coordinate system and the post-processed coordinate system in the description of the experimental setup.

Regarding the definition of x=0D in Fig. 1(a), we have improved the figure so that it is consistent. In the revised manuscript, we have added the following lines in Section 2.1 (Lines 159–163).

It should be noted that in the laboratory setup, the disc is yawed with respect to the y-axis of the coordinate system shown in Fig. 2, resulting in a physical wake deflection in the z-direction. To measure streamwise wake evolution, the laser measurements are therefore performed in the xz-plane of the laboratory coordinate system. For data analysis and presentation, the coordinate system is rotated in post-processing to follow the standard convention in the literature, where yaw occurs about the z-axis and the wake deflects in the y-direction.

2. *Table 1 - please write what w/o disc means. Does it mean with and without disc?*

Reply: The abbreviation "w/o" means *without* the disc. We have removed this short form of 'w/o' and explicitly state "without the disc" in Table 1 in the revised manuscript.

3. *and Line 164: 'Baseline uniform inflow' is unclear. it is unclear what this means - I suggest to have one clear way of terminology*

Reply: Thanks for this comment. We have replaced the word 'baseline uniform inflow' with 'uniform inflow conditions' in the entire manuscript, which refers to the inflow condition when veer vanes are not installed at the tunnel exit. For veer inflow, we refer to them as "veered inflows". For e.g., veered inflow of 10° or 20°.

4. *Line 226 - 'all inflow conditions' , better all three inflow conditions*

Reply: Thanks for the suggestion. Wherever applicable, we have changed 'all inflow conditions' with *all three inflow conditions.*

5. *Fig 4. - There are clear deviation of the veer at z between 0 and -0.2 D wich seem to be caused by the imperfect veer generation. This has to be discussed as it is just in the region where the wakes are measured.*

Reply: Thanks to the reviewer for pointing this out. The localized deviation of the veer profile ("the hump") observed in the region $z/D \in [0, -0.2]$ is indeed a characteristic of the wake generated by the veer-inducing vanes. Physically, the vanes create discrete regions of velocity deficit and lower static pressure. The surrounding freestream flow tends to migrate toward these low-pressure wake regions, causing a localized redistribution of momentum that slightly alters the intended veer profile in the measurement plane. This effect is evident for both the 10° and 20° wind veer models. We emphasize that this deviation is confined to a narrow vertical extent and does not affect the overall imposed veer. We have added a note about this in Section 2.6 (Lines 294–298) of the revised manuscript, where we discuss flow characterization.

As a result of producing wind veer using vanes, a localized deviation in the velocity profile is observed in the region $z/D \in [0, -0.2]$ for both 10° and 20° wind veer cases. This non-uniformity stems from the wakes of the veer-generating vanes; the resulting local low-pressure regions induce a slight migration of the freestream flow, causing a localized distortion of the intended veer profile.

6. *Line 244 - why is the veer reported for x=5D and not like before for 7D*

Reply: We thank the reviewer for identifying this inconsistency. The reporting of the veer at $x/D = 5$ was an oversight; for consistency with the previous discussion of 10° veer model, we have updated this to $x/D = 7$. At this downstream location, the total veer across the porous disc is around 10.81°. In the revised manuscript, this is reflected in the Line 288:

For the 20° wind veer configuration, the actual veer across the porous disc is 14.3° at $x/D = 0$, reducing to around 10.81° at $x/D = 7$.

7. *Line 265 . Sentence wrong: 'As the tower is relatively thicker than the diameter of the porous disc*

Reply: We appreciate the reviewer's correction. Indeed, the sentence phrasing is wrong. Our intention was to highlight the fact that the tower diameter is relatively large in proportion to the 10 cm disc diameter. The thick tower diameter clearly has an influence on wake characteristics. This change is reflected in the revised manuscript in Line 314:

Given the relatively large diameter of the tower in proportion to the disc diameter (with a disc-to-tower diameter ratio of 10) ...

8. *Periodic structures in Figs. 6 and 7 a show that the veer is not constant in y-direction, a plot of veer in y- direction in addition to Fig. 4 c and d is necessary. Here I have problems that these periodic veer structures do not affect the whole results as indicated above this has to be discussed more in this paper. The reader must get convinced that the results remains sensual. It is important to quantify this veer structure, how much is the veer change in your-direction? In the discretization of color calibration does not allow to the the veer imperfection.*

Reply: We thank the reviewer for this comment. Indeed, along the $y-$direction, veer is not constant. We presented veer contours in your earlier major comment #2b, along with some discussion about the wake characteristics of the vane. In the revised manuscript, we have discussed more about this in the new Section 4 *"Limitations of the experimental setup and future work."* We also highlight the veer inflow profiles in the revised manuscript.

9. *Fig 8 the wake center calculation for the kidney shaped cases makes not much sense. In Figs 6 and 7 the wakes are characterized more by two wake centers. Tower and veer generator will have an impact on this.*

Reply: We thank the reviewer for raising this point. For the yawed (and or veer) cases, the wake cross-section deviates from a Gaussian shape and forms a complex wake topology. For such a complex wake structure, the center of mass method is a good metric to track the net lateral and vertical displacement of the wake as a whole. The wake center calculation method employed here follows the methodology of Howland et al. (2016) (see Fig. 6 of their paper) and is commonly used to identify the wake center of complex wake shapes (Heck and Howland, 2025; Bensason et al., 2025). As a result of the tower, there is a downward displacement of the wake, resulting in a systematic downward displacement of the calculated vertical wake center (z_c). Since we did not perform measurements of the tower in isolation (without the disc attached), it is hard to isolate the effect of the tower. Nevertheless, as this vertical bias due to the tower is present in all cases measured, the relative comparison between the control cases and the reference uniform inflow and no-yaw case remains valid. Regarding the vane effect on wake center position: we acknowledge that the vanes introduce localized velocity deficits. However, the wake centroid method is an area-weighted integral of momentum deficit. Since the velocity reduction caused by vanes is small ($< 10\%$ of U_∞) and spatially confined compared to the massive deficit of the disc wake, its contribution to the integral is negligible. The global wake center calculation is dominated by the disc's deficit; therefore, the minor, localized disturbances from the vanes do not materially alter the reported wake center trends.

10. *Fig 8a (no- veer case) shows that the wakes are pushed to the left, is there any reason, I guess this must be an effect of the wind tunnel itself. This strong displacement to the left is not see in the cited publications. The argument : 'This is likely because the laser sheet is not perfectly parallel to the wind tunnel exit plane and is slightly misaligned.' - if this is the reason this is a bad set, which should be redone or calibrated correctly. Such a bias from the set-up must be avoided or taken out. This has to be corrected! I am not convinced that this is only due to the laser sheet setting. As all wakes have this tendency. It is very important to show that this is not due to a flow pattern in the wind tunnel. If it is just a misalignment of a laser, I can not understand that the position changes downstream and becomes maximal at 7D? This looks much more like an advection in this direction! Please clarify this properly.*

Reply: Thank you for this important observation. We addressed this question in your major comment #2a previously.

11. *Furthermore, the estimation method for the wake center after equation 5 appears to be affected by the tower deficit, resulting in an asymmetrical wake (see Fig. 5b, right). This gives rise to a negative bias in the z-direction of the wake centre, as shown in Fig. 8a.Line 287: "Also, it is quite obvious that yawing the disc moves the wake center in the opposite direction of yaw as seen in Fig. 8a, ..." - in Figure 8a in comparison with Fig 8 b and c*

Reply: Thanks to the reviewer for this comment. We addressed this question in your earlier comment #9. In addition, we would like to mention that the primary purpose of showing wake center analysis is to highlight the relative trends between the veer and no-veer cases, which follow a consistent and physically meaningful pattern. We have also revised that section slightly to remove inconsistency in the discussion (Lines 369–373).

12. *Line 310 ff: The wake deficit is not well quantifies by maximum of the deficit. It is better to integrate over the wake area, choosing a threshold. This allow a much better quantification.*

Reply: Thanks to the reviewer for this comment and suggestion. We agree that choosing a single value of maximum wake deficit might introduce bias in results. In the revised manuscript, we quantify the wake deficit using an integral approach. We have calculated the integrated wake deficit and normalized it with the wake area (A_w) and reference velocity (U_{ref}) for each inflow, i.e., $M_x = \frac{\iint \Delta u dy dz}{U_{ref} A_w}$. We define the wake region using a velocity threshold where $\overline{u}/U_{ref} = 0.90$.

In the revised manuscript, we have added a new heatmap (Fig. 10 in the revised manuscript), along with a detailed discussion (Lines 388–409).

13. *The conclusion that 'within each veer case, increasing yaw from 0◦ to 30◦ does not alter the peak deficits ´for me not convincing. I propose to take aa advection model where veer is just advecting the wake in different direction, and compared with the measurements with such a simple advection model.*

Reply: Thanks to the reviewer for this comment. We addressed this question in your major comment #1a

14. *Line 343 '...tion in the CVP (Fig. 10c, '. the end of the brackets is missing*

Reply: Thanks for this observation. The missing bracket has been added in the revised manuscript (Line 427), and the text has been checked for similar typographical errors.

15. *Fig 12 . For veer 20° the background structure are clearly seen in term I - see comments above.*

Reply: Thanks for this observation. Unfortunately, these background structures are an unavoidable consequence of using the veering vanes. We have acknowledged the limitation.

16. *For equation (7) it should be noted that the 1/overbaru is a nontrivial local term, which changes the pattern of Fig 12. This leads to the conclusion of line 412: more entrainment of fluid occurs into the wake from the vertical direction than the spanwise direction." What is not obvious in Fig 12*

Reply: Thanks for this comment. The $\frac{1}{\overline{u}}$ factor in Eq. 7 is spatially varying and amplifies the contributions in the lower-velocity wake core, which is why the relative magnitudes of terms in the integrated budget (Fig. 14 in the revised manuscript) may differ from what one might infer visually from the contour plots in Fig. 12. Moreover, the purpose of Fig. 13 was to show the contributions from each term and regions where momentum recovery is benefited or vice versa. A higher vertical entrainment of momentum (red regions) can still be seen in second column tiles in Fig. 13, which shows the contours of $-\overline{w}\frac{\partial \overline{u}}{\partial z}$.

17. *Notation of case Fig 13 WV10Y30. This notation is introduced and explained later in Fig 16 $WV\phi Y\theta$. This is a bad style - see comments above to use throughout the whole paper clear well defined notions.*

Reply: Thanks to the reviewer for this observation. In the revised manuscript, we have moved the notation explanation $WV\phi Y\theta$ in the caption of Fig. 9, where we first use them.

18. *Fig 14 the calibration bar for TKE on top is unusually.*

Reply: Perhaps the reviewer means that the colorbar in Fig. 14 is too small. Thanks for this observation. We have made a new figure with a thicker colorbar in the revised manuscript (see Fig. 15).

19. *Fig 15 I do not see why the veer specification are given two time for each figure part.*

Reply: Thanks to the reviewer for this comment as well. We have removed Fig. 15 in the original manuscript and replaced it with the terms of the TKE budget equation (based on your next comment).

20. *Line 430 the statement 'The increase in TKE for the veered cases can be explained by looking at the profiles of shear production of turbulence' is not well documented. It is hard to compare Fig. 14 with Figure 15 due to different presentations. Taking the case, no veer no yaw and x/D=3 - on sees that the production is maximal at the sides of the rotor plane, the TKE is maximal at the lower part of the wake, contradicting the statement. For the veered cases the double structure of the production is not seen for TKE. This comparison should be worked out better, from the presentation as well as from the discussion. Overall this discussion of turb. production and TKE is not good, it is very superficial.*

Reply: We thank the reviewer for pointing out the inconsistencies in our initial comparison. To better understand the mechanism leading to faster wake recovery, we have now performed a budget analysis of the turbulent kinetic energy (TKE). The time-averaged TKE budget equation can be written as (Pope, 2001):

$$\underbrace{\overline{u}_j\frac{\partial k}{\partial x_j}}_{\text{Advection }(\mathcal{A}_k)} = \underbrace{-\overline{u_i'u_j'}\frac{\partial \overline{u}_i}{\partial x_j}}_{\text{Production }(\mathcal{P}_k)} \underbrace{-\frac{\partial}{\partial x_j}\left(\frac{1}{2}\overline{u_i'u_i'u_j'}\right)}_{\text{Turbulent Transport }(\mathcal{T}_k)} \underbrace{+\nu\frac{\partial^2 k}{\partial x_j^2}}_{\text{Viscous Diffusion }(\mathcal{V}_k)} - \underbrace{\nu\overline{\frac{\partial u_i'}{\partial x_j}\frac{\partial u_i'}{\partial x_j}}}_{\text{Dissipation }(\varepsilon_k)} \tag{2}$$

We evaluate the terms of Eq. 2 on $yz-$planes at $x/D = 5$. Given the sufficiently high Reynolds number, the viscous diffusion term ($\mathcal{V}_k$) can be ignored (also done in TKE budget analysis of many LES-based studies, see Klemmer and Howland (2024)). The dissipation term (ε_k), on the other

hand, cannot be measured by PIV because the spatial resolution cannot resolve the Kolmogorov scales. Consequently, our analysis only considers the contribution from advection ($\mathcal{A}_k$), production ($\mathcal{P}_k$), and turbulent transport ($\mathcal{T}_k$) terms. The reviewer is requested to refer Section 3.4 (Lines 517–540)

To make the figures comparable, we have made the figures now with the same style. To answer the reviewer's comment about the TKE being higher in the lower-half of the disc and production being higher on the sides, we would like to highlight that the TKE considers the effect of all Reynolds normal stresses ($\overline{u'u'}$, $\overline{v'v'}$, and $\overline{w'w'}$) and is a "net result", of the balance between the different terms in the budget equation, such as advection, production, turbulent transport, and dissipation. The *production* term, on the other hand, describes the process by which kinetic energy from the mean flow is transferred to the fluctuating velocity fields, and in our contours on $yz-$plane, we do not consider the streamwise fluctuations, $\overline{u'u'}$ (because we cannot compute $\frac{\partial u}{\partial x}$ in the $yz-$plane) which is primary contributor to TKE enhancement near the tower region (and dominates other Reynolds stresses terms) and that is why it appears higher in the TKE contours t $x/D = 3$. Moreover, the presence of the tower, which acts as a bluff body, also has a clear effect in concentrating TKE in the bottom half due to large velocity fluctuations. The production term does not have the contribution from $\overline{u'u'}$. Moreover, all of the TKE cannot be explained by the production term.

21. *Line 452 - please specify more precisely the location of hub height zT and lateral position yT. Are the turbines aligned with the wind speed direction at hub height?*

Reply: The center of the disc is defined at the origin of the coordinate system, (y_T, z_T)=$(0, 0)$. Yes, the disc is aligned with the wind speed direction at hub height. To clarify this for the reader, we have updated that sentence in Lines 555–556 in the revised manuscript to explicitly define the disc center location and its orientation.

22. *Line 450 ff the power comparison is not acceptable. Wind turbines are operating in general not aligned with the direction of the incident flow. An integration over different lateral positions would be much more adequate for the investigated cases. In this analysis also the experimental inaccuracy becomes important, like for the WV0Y0 case the center is displaced as shown in Fig 5b. This inhomogeneity of the wind tunnel has to be taken into account. The presented results indicate that the WV0Y0 cases of Fig 16 are affected by the drift of the wake to the left even for this symmetric case. Averaging over different y-positions could scope with this insufficiency of the wind tunnel. The whole discussion of AP has to be revised, this is not acceptable. I also fear that the veer structure of the gird will have an effect of AP as the locations of the wakes seem to be impacted by these - see for example Fig 7c.*

Reply: If we understand the reviewer correctly, they are basically asking us to show the integration of the available power variation in lateral direction in Fig. 16. This is precisely what we have shown in Fig. 16 and 17 (in the revised manuscript they are Fig. 17 and 18, respectively): it is not a point-wise comparison but rather an area integrated quantity evaluated over a sliding lateral window. In other words, to compute the f_{AP}, we integrate:

$$f_{AP}(x_T, y_T, z_T) = \frac{\iint_G U(x_T, y, z)^3 \, dy \, dz}{\iint_G U_{\text{in}}(y, z)^3 \, dy \, dz} \tag{3}$$

where G denotes the frontal projection of the porous disc centered at the candidate turbine location (x_T, y_T, z_T). The integration window is then traversed laterally across the wake, producing the

profiles shown in Fig. 17 and contours maps in Fig. 18. This way, it takes into account the inhomogeneity of the wind tunnel and allows readers to evaluate optimal positioning strategies. Our discussion of available power is consistent with many other studies that have used it as a metric to investigate the power available for the downwind turbine (e.g., Vollmer et al. (2016); Zong and Porté-Agel (2020); Bossuyt et al. (2021); Bensason et al. (2025)).

We recognize that our original figure caption and accompanying text may not have conveyed this procedure clearly. In the revised manuscript, we have changed the relevant passages to make this clear and avoid any confusion. Please see Lines 550–557, along with captions of Fig. 17 and 18 in the revised manuscript.

Or if the reviewer is asking for a spatially averaged value of the available power coefficient in the lateral direction within the wake area, then the Table 1 shows a single spatially averaged value of f_{AP} for each case by integrating the profiles in Fig. 16 across the full wake span (covering the entire lateral domain) at three downstream locations. The WV0Y0 and WV10Y0 exhibit similar values at all locations. This is because the f_{AP} profiles for the former case is below the latter case when $y/D < -0.2$. For $y/D > -0.2$, the reverse is the case. Due to this reason, it averages out the effect and relatively similar values are seen. A higher value of f_{AP} is seen for the WV20Y0 case compared to other non-yawed cases. This clearly shows that veer does not merely steer the wake, but actively enhances the net energy recovery across the domain.

Case	$x/D = 3$	$x/D = 5$	$x/D = 7$
WV0Y0	0.53	0.58	0.63
WV0Y30	0.63	0.68	0.73
WV10Y0	0.53	0.58	0.62
WV10Y30	0.64	0.69	0.71
WV20Y0	0.55	0.63	0.70
WV20Y30	0.66	0.73	0.78

Table 1: Laterally averaged values of the coefficient of available power of each profile in Fig. 16 for three downstream locations.

23. *Fig 17 rearrange the plots. Up to here, it was always started with no veer - quite often vertical direction are the veer cases and horizontal the yaw cases - work out one scheme used in the whole paper consistently. As stated above an integration over the cases of Fig 17 are interesting and should be worked out.*

Reply: Thanks to the reviewer for this comment. Wherever possible, we have adhered to the convention of veer cases in the vertical direction and yaw cases in the horizontal direction. This convention is not adopted in the momentum budget analysis because of visual clarity.

Reviewer #3

The article discusses the effects of wind veer on wind turbine wakes and available power. The manuscript is well-written and the presented results have valuable potential within both the wind energy community and fundamental wake research. However, some comments should be addressed prior to publication as provided below:

Reply: We thank the reviewer for acknowledging our work and finding the manuscript well-written. Below, we have provided our responses to your questions.

Specific comments

1. *Lines 19-29: Veering is stated to be "the change in wind direction with height" and an example maximum of rotor diameter is mentioned. However, the extent to which height-relative veering would impact operational turbines is not clear. For example:*

   (a) *In Line 25, the statement "At such heights, wind veer can be substantial..." does not follow a description of turbine heights, only mention of the max rotor diameter of 260 m. Specific/quantified examples of typical turbine heights from ground (ie. hub height, rotor swept extents) and height-relative veering would clarify physical scale and strengthen motivation.*

Reply: Thanks to the reviewer for pointing this out. Indeed, this was not very clear. In the revised manuscript, we have rephrased this part as follows (please see Lines 23–28):

The largest commercially deployed wind turbine to date—the SG 14-222 DD at Moray West offshore wind farm in Scotland—features a rotor diameter of 222 m and a power capacity of 14.7 MW. With a hub height of approximately 140 m, the rotor swept area extends from roughly 30 m to 250 m above mean sea level. Prototypes of even higher-rated turbines, exceeding 20 MW, are currently in various stages of development, which will result in even taller structures. As the rotor spans of modern WTs are reaching 200–300 m, turbines operating across such vertical extents can experience a substantial level of wind veer.

1. (b) *Height-relative turning $D(z)$ is reported in the Van Ulden and Holtslag (1985) study as the angle of turning compared to the height $z = 20$ m from the ground. Based on their Table 2 and Equation 51, it appears that turning angle variation per-meter (i.e.$\partial(D(z))/\partial z$) are greater at lower elevations and begin to asymptote at greater heights. Thus, one may argue that veering across just the rotor swept extent for an operational turbine may be more minimal at greater heights. Alongside clarification of turbine physical extents for Comment 1(a), discussion of possible ranges in typical wind-turning estimates across the rotor of a typical turbine may also strengthen motivation.*

Reply: Thanks to the reviewer for this comment. In the revised manuscript, we have modified the end of the first paragraph of Introduction to highlight this effect as follows (Lines 28–33):

Observations at Cabauw observatory indicate wind veering up to 40° over the lowest 200 m of the atmosphere, i.e., veer change of 0.22° m^{-1} (Van Ulden and Holtslag, 1985). Furthermore, wind veer was observed to occur more than 70% of the time over the course of a year in offshore environments with an average veer of 0.07° m^{-1} (Bodini et al., 2019). For a modern turbine of

200 m rotor diameter, this results in wind veer of $\sim 18^\circ$ across the rotor, thus, highlighting the need to account for its effect on WT wake structure and evolution.

2. *Line 33: "Large-eddy simulation (LES) is the most preferred way to study wind turbine wakes due to its ability to resolve large-scale turbulent structures and accurately capture unsteady wake dynamics (Xie and Archer, 2017)." This should be restated to remove subjectivity and to be more precise. Specifically, one could argue that LES is not always the most preferred way to study wind turbine wakes when small-scale features desired.*

Reply: We agree with the reviewer that the original phrasing was too subjective. In the revised manuscript, this change is reflected in Lines 37–39:

Large-eddy simulation (LES) is a widely adopted high-fidelity approach due to its faithful prediction of unsteady dynamics and its ability to resolve dominant large-scale turbulent structures that govern wake evolution (Xie and Archer, 2017).

3. *Lines 103-112: Expanded discussion on porous disks is needed to motivate why/how they are used as turbine analogs, as well as the effects/consequences of porosity and void location/distribution on turbine wake-mimicking behavior.*

Reply: We have expanded the discussion on porous discs in the main text to better motivate their use as turbine analogs. The following text has been added (Lines 105–130):

The choice of a non-rotating porous disc is motivated by its simplicity and ease of implementation in wind tunnel experiments, as well as the ability to readily adjust the disc porosity (β), defined as the ratio of open area to the total disc area, to match the thrust coefficient of an operating wind turbine. Steiros and Hultmark (2018) derived a simple relation between the drag coefficient (C_D) and β using potential flow theory and momentum conservation, and experimentally validated it against a range of disc porosity values. Since the seminal work of Castro (1971), who investigated flow through perforated discs, porous discs have been widely researched as analogs for wind turbines. For example, Sforza et al. (1979) employed perforated discs to emulate wind turbine wakes. Since then, several studies have utilized porous discs for a faithful representation of wake characteristics. Primarily, two types of discs have been employed in wind tunnel studies: uniform porous disc where the spacing in the mesh is uniform throughout (Aubrun et al., 2013; Lignarolo et al., 2016), and a non-uniform porous disc with porosity varying radially to reproduce the realistic loading distribution (Howland et al., 2016; Camp and Cal, 2016, 2019; Aubrun et al., 2019; Neunaber et al., 2021; de Jong Helvig et al., 2021; Vinnes et al., 2022, 2023; Öztürk et al., 2023; Bourhis and Buxton, 2024). These studies have demonstrated that porous discs can reproduce the key feature of turbine wake, particularly in the far wake. In particular, Aubrun et al. (2013) found that beyond $x/D > 3$, the wakes of a rotating turbine and a porous disc exhibit similar characteristics. Likewise, Lignarolo et al. (2016) reported comparable wake expansion and energy extraction between a wire mesh disc and a wind turbine under low turbulence when matched in diameter and thrust coefficient. Studies have also shown that higher-order two-point statistics of wind turbine models can be replicated by porous discs (Neunaber et al., 2021; Vinnes et al., 2022). The most critical parameter in the porous disc is the disc porosity that essentially determines the flow resistance, and hence C_D. It was shown by Bourhis and Buxton (2024) experimentally that wake evolution is different for discs with varying porosity and thrust coefficients and strongly depends on the

freestream turbulence and integral length scale in the ambient flow. With increasing disc porosity, the wake shifts from the periodic von-Kármán vortex shedding pattern to the regime where this is absent (Cicolin et al., 2024). Apart from the disc porosity, Theunissen and Worboys (2019) found that even for the same porosity, the hole topology can have significant changes on the near-wake characteristics and drag coefficient, thus highlighting the need to properly choose the design of the porous disc. In summary, porous discs—when carefully designed to match the thrust coefficient of an operating wind turbine—have been shown to faithfully reproduce key wake characteristics, making them a practical and well-validated tool for parametric wind tunnel investigations.

4. *Section 2.2: Porous disc and wind veer model*

   (a) *Further description and/or an annotated diagram of the disk design is suggested beyond references to diameter and porosity ratio. Including information on porosity void distribution and void dimensions throughout the disk is advised since this is known to affect wake features. It is also suggested to include the disk position distance in x from the tunnel exit.*

Reply: We have replaced the Fig. 2 in the original manuscript with the following figure that also describes the dimensions of the porous disc.

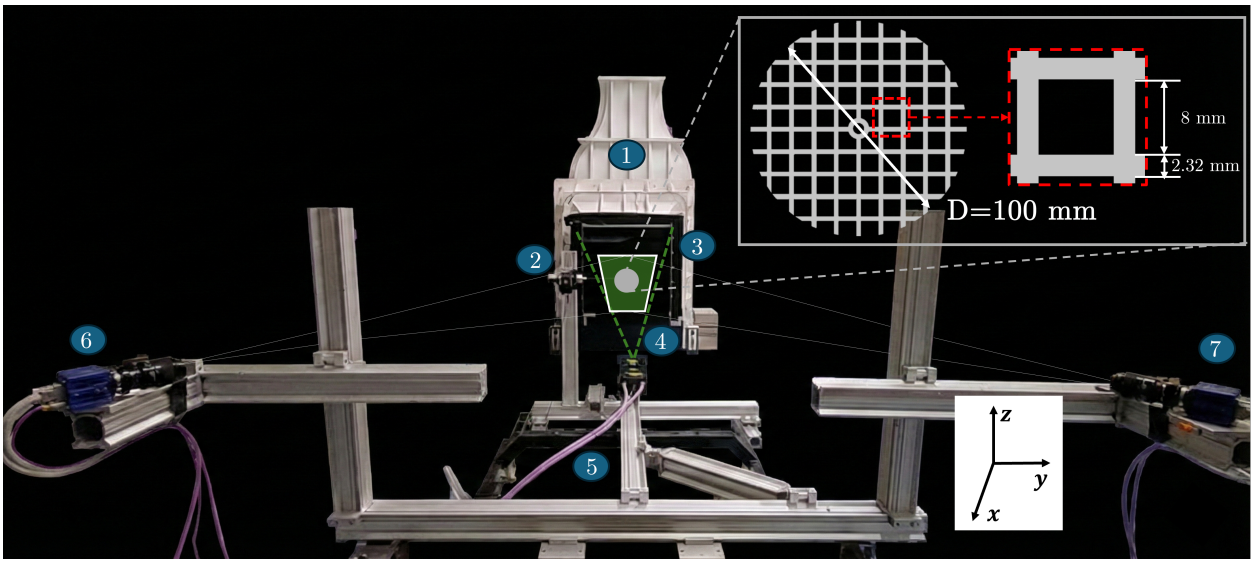

Figure 8: Photograph of the experimental setup in the W-Tunnel for measuring cross-stream wake planes. The key labeled components are as follows: 1. Exit of the W-tunnel; 2. Rotation stage on which a porous disc is mounted; 3. Wind veer model installed at the exit of the wind tunnel; 4. Laser sheet emanating from the laser (span of the sheet marked by dashed green lines); 5. Traverse system; 6: Camera 1; 7: Camera 2. The field of view (FOV) is denoted by a filled green trapezoid. The porous disc is shown as a solid gray circle. The inset figure shows the dimensions of the porous disc along with the void dimensions. The coordinate system is shown on the bottom right.

4. (b) *Discussion of the PIV plane coordinate system should be revisited/edited as it appears to be somewhere misrepresented. For example, the diagram in Fig. 1b suggests that the*

streamwise planes are situated in xz, but reported plane orientation in the caption and text is xy.

Reply: Thanks to the reviewer for pointing this out. Reviewer #2 also had a similar question and was addressed to his minor comments #1 (Pages 10–11).

4. *(c) Visual clarification on orientation of veering blades would be helpful. For example, is the veering blade length in y?*

Reply: In the revised manuscript, we have added the drawing details of the wind veer vane model of 10°. We have modified Fig. 3 in the original manuscript to the figure below. Furthermore, the CAD models of both veering vanes will be provided as supplementary material for researchers wishing to replicate these experimental conditions.

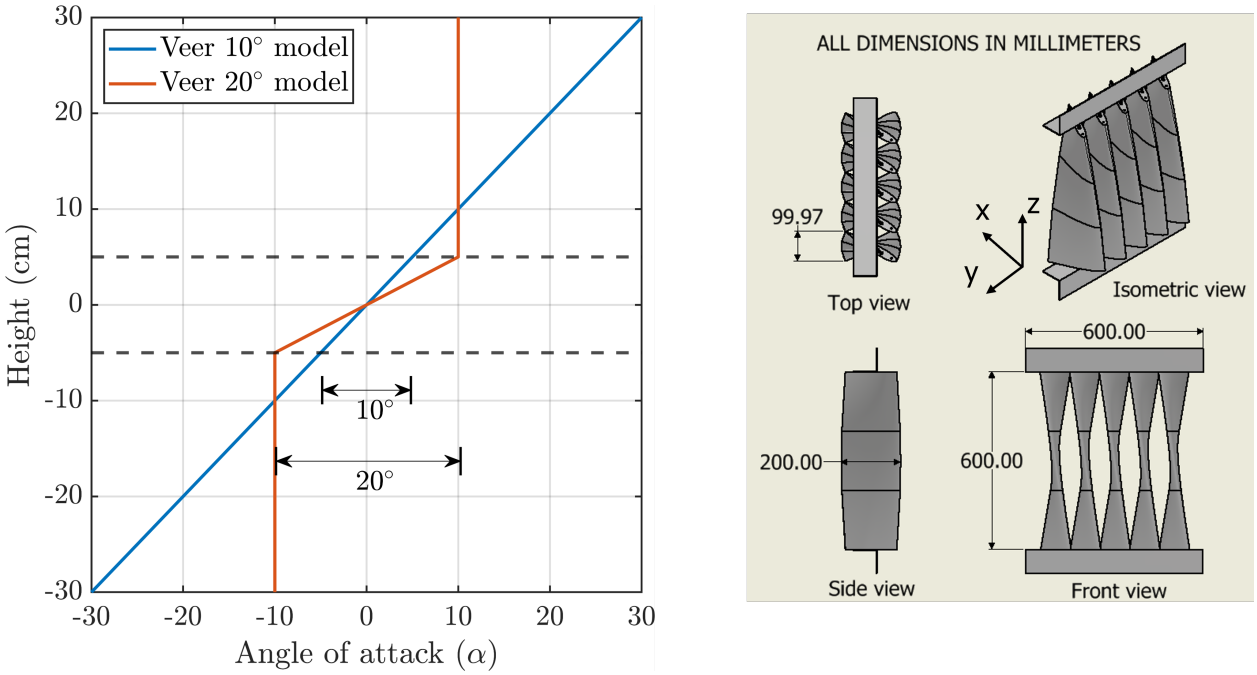

Figure 9: (Left figure) Variation of angle of attack of the NACA airfoil for wind veer model of 10° (blue line) and 20° (red line). The dashed horizontal line represents the top and bottom extent of the disc, such that a total of 10° and 20° veer is generated from the two models, respectively; (Right figure) Different views of the wind veer model for generating a veer of 10° installed at the exit of the wind tunnel. The leading-edge portion of the model is located inside the wind tunnel, while the trailing-edge portion extends outside. A similar model that generates a wind veer of 20° (not shown here) is also tested.

5. *Section 2.4 Flow measurement system: What convergence analysis was done to ensure that 100 snapshots was sufficient? While not impossible to achieve at N=100, many more images are typically needed for PIV data to fully converge—especially for terms involving velocity fluctuations (e.g. momentum, TKE). Uncertainty analysis through σ_u (Section 2.5) can be an unreliable measure of PIV data "goodness" in the case of non-converged fluctuations.*

Reply: Thanks to the reviewer for this comment. Reviewer #1 had a similar comment and is addressed in the answer to the Reviewer's comment #2 (see Fig. 2 and related discussion on pages 2 and 3 of this rebuttal).

6. *Section 2.6 Flow characterization*

   (a) *Line 232: "A minor spanwise velocity component of approximately 2 % is observed, likely caused by a slight misalignment of the laser sheet with the wind tunnel exit." This comment leads to two questions:*

      i. *If this was due to a laser sheet misalignment, why would the profile exhibit a central hump of higher magnitudes bounded by $v/U_{ref} = 0$ rather than linear asymmetry across the profile? Specifically, above $z/D = 0.5$ and under the legend (only slightly visible – see Technical Corrections 3a), it appears that $v/U_{ref} = 0$.*

      ii. *Could non-zero spanwise and/or vertical velocities in the "clean" case be a result of the open jet-type wind tunnel? Was the w velocity component also plotted for reference?*

Reply: We thank the reviewer for this important observation. A similar question was asked by Reviewer #2 and is addressed in the answer to Reviewer's major comment #2a (Page 8). Additionally, Fig. 4 in the revised manuscript has been updated to include the w-velocity component and the requested aesthetic improvements.

6. *(b) It may be helpful to include in-text how veer was calculated for Fig. 4.d.*

Reply: Thanks for this suggestion. We believe the reviewer is talking about the dashed magenta line in Fig. 4d. We have added the following sentence on how the ideal wind veer is calculated in Lines 289–291.

The dashed magenta line shows the ideal wind veer profile. It is calculated based on the fact that wind veer is the linear function of vertical coordinate, i.e., $f(z) = A(z/z_{max})$, where A represents the maximum veer amplitude at the domain boundaries $z = \pm 0.5$.

6. *(c) Line 241: "Despite this, the turbulence intensity across the disc area remains below 2 % at all measured streamwise locations for both veered cases. . . ". This does not appear to be entirely true for the 10∘ veering case at $x/D = 7$.*

Reply: Thanks to the reviewer for pointing this out. Indeed, around the disc edges, the TI is slightly higher than 2 % for the 10° veer case at $x/D = 7$. This is mainly attributed to the design of the 10 ° veering vane that results in more turbulence mixing in the wake. We have modified that sentence to reflect this change (Lines 284–286).

Despite this, the turbulence intensity across the disc area remains below 2.5 % at all measured streamwise locations for both veered cases, indicating relatively low levels of added turbulence by the veering vanes.

Technical corrections

1. *In-text citations should be corrected throughout the manuscript to ensure parenthetical citations are not in direct reference form. For example, in Line 68: "The aerodynamics of yawed wind turbines were first studied experimentally by (Grant et al., 1997) and (Grant and Parkin, 2000)."*

Reply: Thanks to the reviewer for this observation. The in-text citations have been checked and fixed in the revised manuscript.

2. *Velocity variables in axis labels and text should be edited to denote averaging where appropriate and remain consistent throughout. For example, contours and Fig. 4 profiles show velocity as lower-case u with no over-bar, but streamwise velocity is also referred in text as U_x and u.*

Reply: Thanks to the reviewer for this observation. Wherever applicable throughout the text, streamwise velocity, spanwise velocity, and vertical velocity are now denoted as $\overline{u}$, $\overline{v}$, and $\overline{w}$.

3. *It is suggested to eliminate phrases such as "As expected. . . ", "As anticipated. . . " from the manuscript without citing the source(s) of the expected outcome. If results mimic behavior seen in other studies, it is best to cite those studies rather than assume reader knowledge.*

Reply: Thanks to the reviewer for this suggestion. In the revised manuscript, we refrain from using such phrases and properly cite the source of the expected outcome.

4. *Corrections to Fig 4:*
   (a) *Legends should not block profiles. As an additional aesthetic suggestion: consider consistent legend positioning in subplots and/or minimize repetitive legends when colors/linestyle represent the same quantities throughout.*
   (b) *Axis ranges for u/U_{ref} should be corrected to make all reported data visible. Also, minimizing unused high-range space would more clearly show variations between "clean" and veering cases.*

Reply: Thanks for these suggestions as well. The Fig. 4 in the revised manuscript has been improved based on your suggestions (see Page 14 in the revised manuscript).

4. *Lines 197-199 are redundant as the phrase "It should be noted. . . " is used in two consecutive sentences.*

Reply: This has been removed in the revised manuscript (see Lines 235–237).

5. *Line 265-268: "As the tower is relatively thicker than the diameter of the porous disc (with a disc-to-tower diameter ratio of 10). . . ". This statement may intend to read differently, but in its current form is self contradictory and unclear.*

Reply: Thanks for this observation. Indeed, this sentence was meant to be read differently. We have edited this sentence properly in the revised manuscript (see Line 314).

6. *Line 322: It would be helpful to follow the statement of ". . . as reported in multiple field experiments. . . " with direct citation(s) where this is reported.*

Reply: Thanks for this observation. We have added a few references for this sentence now. Please see Lines 406–407 in the revised manuscript.

7. *Line 328 "As also discussed in Section 3.1,. . . ": No reference to vortex pairs was made in Section 3.1.*

Reply: Thanks for pointing this out. We have removed the reference to vortex pairs in that sentence (Line 412 in the revised manuscript).

References

Archer, C. L. and Vasel-Be-Hagh, A.: Wake steering via yaw control in multi-turbine wind farms: Recommendations based on large-eddy simulation, Sustainable Energy Technologies and Assessments, 33, 34–43, 2019.

Aubrun, S., Loyer, S., Hancock, P. E., and Hayden, P.: Wind turbine wake properties: Comparison between a non-rotating simplified wind turbine model and a rotating model, Journal of Wind Engineering and Industrial Aerodynamics, 120, 1–8, 2013.

Aubrun, S., Bastankhah, M., Cal, R. B., Conan, B., Hearst, R. J., Hoek, D., Hölling, M., Huang, M., Hur, C., Karlsen, B., et al.: Round-robin tests of porous disc models, in: Journal of Physics: Conference Series, vol. 1256, p. 012004, IOP Publishing, 2019.

Bastankhah, M., Shapiro, C. R., Shamsoddin, S., Gayme, D. F., and Meneveau, C.: A vortex sheet based analytical model of the curled wake behind yawed wind turbines, Journal of Fluid Mechanics, 933, A2, 2022.

Bensason, D., Sciacchitano, A., and Ferreira, C.: On the wake re-energization of the X-Rotor vertical-axis wind turbine via the vortex-generator strategy, Wind Energy Science, 10, 2137–2159, 2025.

Bodini, N., Lundquist, J. K., and Kirincich, A.: US East Coast lidar measurements show offshore wind turbines will encounter very low atmospheric turbulence, Geophysical Research Letters, 46, 5582–5591, 2019.

Bossuyt, J., Scott, R., Ali, N., and Cal, R. B.: Quantification of wake shape modulation and deflection for tilt and yaw misaligned wind turbines, Journal of Fluid Mechanics, 917, A3, 2021.

Bourhis, M. and Buxton, O.: Influence of freestream turbulence and porosity on porous disk-generated wakes, Physical Review Fluids, 9, 124 501, 2024.

Camp, E. H. and Cal, R. B.: Mean kinetic energy transport and event classification in a model wind turbine array versus an array of porous disks: Energy budget and octant analysis, Physical Review Fluids, 1, 044 404, 2016.

Camp, E. H. and Cal, R. B.: Low-dimensional representations and anisotropy of model rotor versus porous disk wind turbine arrays, Physical Review Fluids, 4, 024 610, 2019.

Castro, I.: Wake characteristics of two-dimensional perforated plates normal to an air-stream, Journal of Fluid Mechanics, 46, 599–609, 1971.

Churchfield, M. J. and Sirnivas, S.: On the effects of wind turbine wake skew caused by wind veer, in: 2018 wind energy symposium, p. 0755, 2018.

Cicolin, M., Chellini, S., Usherwood, B., Ganapathisubramani, B., and Castro, I. P.: Vortex shedding behind porous flat plates normal to the flow, Journal of Fluid Mechanics, 985, A40, 2024.

de Jong Helvig, S., Vinnes, M. K., Segalini, A., Worth, N. A., and Hearst, R. J.: A comparison of lab-scale free rotating wind turbines and actuator disks, Journal of Wind Engineering and Industrial Aerodynamics, 209, 104 485, 2021.

Englberger, A., Dörnbrack, A., and Lundquist, J. K.: Does the rotational direction of a wind turbine impact the wake in a stably stratified atmospheric boundary layer?, Wind Energy Science, 5, 1359–1374, 2020a.

Englberger, A., Lundquist, J. K., and Dörnbrack, A.: Changing the rotational direction of a wind turbine under veering inflow: a parameter study, Wind Energy Science, 5, 1623–1644, 2020b.

Heck, K. S. and Howland, M. F.: Coriolis effects on wind turbine wakes across neutral atmospheric boundary layer regimes, Journal of Fluid Mechanics, 1008, A7, 2025.

Howland, M. F., Bossuyt, J., Martínez-Tossas, L. A., Meyers, J., and Meneveau, C.: Wake structure in actuator disk models of wind turbines in yaw under uniform inflow conditions, Journal of renewable and sustainable energy, 8, 2016.

Klemmer, K. S. and Howland, M. F.: Momentum deficit and wake-added turbulence kinetic energy budgets in the stratified atmospheric boundary layer, Physical Review Fluids, 9, 114 607, 2024.

Lignarolo, L. E., Ragni, D., Ferreira, C. J., and van Bussel, G. J.: Experimental comparison of a wind-turbine and of an actuator-disc near wake, Journal of Renewable and Sustainable Energy, 8, 2016.

Narasimhan, G., Gayme, D. F., and Meneveau, C.: An extended analytical wake model and applications to yawed wind turbines in atmospheric boundary layers with different levels of stratification and veer, Journal of Renewable and Sustainable Energy, 17, 2025.

Neuhaus, L., Berger, F., Peinke, J., and Hölling, M.: Exploring the capabilities of active grids, Experiments in Fluids, 62, 130, 2021.

Neunaber, I., Hölling, M., Whale, J., and Peinke, J.: Comparison of the turbulence in the wakes of an actuator disc and a model wind turbine by higher order statistics: A wind tunnel study, Renewable Energy, 179, 1650–1662, 2021.

Öztürk, B., Hassanein, A., Akpolat, M. T., Abdulrahim, A., Perçin, M., and Uzol, O.: On the wake characteristics of a model wind turbine and a porous disc: Effects of freestream turbulence intensity, Renewable Energy, 212, 238–250, 2023.

Pope, S. B.: Turbulent flows, Measurement Science and Technology, 12, 2020–2021, 2001.

Rajasekara Babu, K., Hu, G., Noack, B. R., and Kwok, K.: From active grids to fan-array wind generators: A review of turbulence generation, control, and artificial intelligence integration in wind tunnels, Physics of Fluids, 37, 2025.

Sciacchitano, A. and Wieneke, B.: PIV uncertainty propagation, Measurement Science and Technology, 27, 084 006, 2016.

Sforza, P., Stasi, W., Smorto, M., and Sheerin, P.: Wind turbine generator wakes, in: 17th Aerospace Sciences Meeting, pp. 1979–113, AIAA, 1979.

Steiros, K. and Hultmark, M.: Drag on flat plates of arbitrary porosity, Journal of Fluid Mechanics, 853, R3, 2018.

Theunissen, R. and Worboys, R.: Near-wake observations behind azimuthally perforated disks with varying hole layout and porosity in smooth airstreams at high Reynolds numbers, Journal of Fluids Engineering, 141, 051 108, 2019.

Van Ulden, A. P. and Holtslag, A. A.: Estimation of atmospheric boundary layer parameters for diffusion applications, Journal of Applied Meteorology and Climatology, 24, 1196–1207, 1985.

Vinnes, M. K., Gambuzza, S., Ganapathisubramani, B., and Hearst, R. J.: The far wake of porous disks and a model wind turbine: Similarities and differences assessed by hot-wire anemometry, Journal of Renewable and Sustainable Energy, 14, 2022.

Vinnes, M. K., Neunaber, I., Lykke, H.-M. H., and Hearst, R. J.: Characterizing porous disk wakes in different turbulent inflow conditions with higher-order statistics, Experiments in Fluids, 64, 25, 2023.

Vollmer, L., Steinfeld, G., Heinemann, D., and Kühn, M.: Estimating the wake deflection downstream of a wind turbine in different atmospheric stabilities: an LES study, Wind Energy Science, 1, 129–141, 2016.

Zong, H. and Porté-Agel, F.: A point vortex transportation model for yawed wind turbine wakes, Journal of Fluid Mechanics, 890, A8, 2020.